



Virginia Commonwealth University
VCU Scholars Compass

Theses and Dissertations


Graduate School

2019

Searching for Clean Observables in $B \rightarrow D^* \tau \bar{\nu}_\tau$ Decays

Michael D. Williams Jr.
Virginia Commonwealth University

Follow this and additional works at: <https://scholarscompass.vcu.edu/etd>

 Part of the [Atomic, Molecular and Optical Physics Commons](#), [Elementary Particles and Fields and String Theory Commons](#), [Other Physics Commons](#), and the [Quantum Physics Commons](#)

© The Author

Downloaded from

<https://scholarscompass.vcu.edu/etd/5885>

This Thesis is brought to you for free and open access by the Graduate School at VCU Scholars Compass. It has been accepted for inclusion in Theses and Dissertations by an authorized administrator of VCU Scholars Compass. For more information, please contact libcompass@vcu.edu.

©Michael David Williams, May 2019

All Rights Reserved.

Acknowledgements

I would like to thank Virginia Commonwealth University for affording me the opportunity to pursue higher education. I would like to thank my peers and the professors in the physics department who have spent countless hours with me in order for me to hone my craft and become a better student, researcher, and person. I would like to thank my committee members, Dr. Prok and Dr. Witten for their countless hours of time and support given to me throughout this thesis. This project would not have been possible without my advisor, Dr. Duraisamy. I am deeply indebted and eternally grateful. I would also like to thank my three sisters, Amanda, Stephanie, and Meagan, for their never ending love throughout my life that has allowed me to get to where I am. Without the constant reaffirmation that my parents would always be there, I would have faltered long ago. I owe everything to them and I hope I continue to make them proud. Finally, I would like to thank you, the reader, for taking the time to read my thesis. Thank you.

Sincerely,

Michael "David" Williams

TABLE OF CONTENTS

Chapter	Page
Acknowledgements	ii
Table of Contents	iii
List of Tables	iv
List of Figures	vi
List of Abbreviations	viii
Abstract	ix
Introduction	1
1 Theoretical Background	3
1.1 The Standard Model	3
1.1.1 Leptons	4
1.1.1.1 Spin	4
1.1.1.2 Helicity	5
1.1.1.3 Parity	5
1.1.1.4 Anti-Leptons	6
1.1.2 Quarks	6
1.1.3 Gauge/Scalar Bosons	7
1.1.3.1 The Electromagnetic Force	7
1.1.3.2 The Weak Force	8
1.1.3.3 The Strong Force	9
1.1.4 Hadrons	9
1.1.4.1 Mesons	10
1.1.5 Physics Beyond the Standard Model	11
1.2 <i>B</i> Mesons	11
1.2.1 CKM Mixing Matrix	13
1.2.2 CP Violation	13
1.2.3 Lifetimes and Cross Sections	15

1.2.3.1	The Golden Rule and The Feynman Rules for a Toy Model	17
1.3	Fields and Propagators	18
1.3.1	Charged Current and Neutral Current	18
1.3.2	Propagators	19
1.3.2.1	Scalar Fields	20
1.3.2.2	Pseudoscalar Fields	20
1.3.2.3	Vector Fields	21
1.3.2.4	Axial Vector Fields	21
1.3.2.5	Tensor Fields	22
2	Formalism of $\bar{B} \rightarrow D^{(*)}\ell^{-}\nu_{\ell}$	23
2.1	Discussion of $B \rightarrow D\ell\nu_{\ell}$	24
2.2	Discussion of $B \rightarrow D^{*}\ell\nu_{\ell}$	24
2.2.1	Form Factors	25
2.3	Angular Observables in $\bar{B} \rightarrow D^{*}\ell\nu_{\ell}$	29
3	Numerical Analysis	31
3.1	Region Plots	33
3.2	Moving Forward	35
3.2.1	Clean Observables	36
3.3	Discussion	37
	Bibliography	39

LIST OF TABLES

Table		Page
1	Above table shows each quark and its symbol, mass, electric charge (Q), baryon number (B), strangeness (S), charmness (C), bottomness \tilde{B} , and topness (T)[13][16]	7
2	The above table shows a few common mesons, their quark composition, mass, electric charge (Q), strangeness (S), charmness (C), and bottomness \tilde{B} [13][16][18][19][21].	10
3	The above table shows the different possible B Mesons, their quark content, and electric charges.	11
4	The above table shows the different possible D Mesons and their quark content and electric charges. It should be noted that while the first two and last two entries have the same quark content, the last two entries have different rest masses, total angular momenta, and the last two also have much shorter lifetimes than their counterparts.	12
5	The above table denotes the types of mesons and the corresponding value of their spin (S), orbital angular momentum (L), parity transformation (P), total angular momentum (J), and the combination of the total angular momentum with the parity transformation (J^P).	22
6	The above table shows the values of the form factors during the transition $B \rightarrow D$	29
7	The above table shows the values of the form factors during the transition $B \rightarrow D^*$	29
8	The above table shows the masses of the W boson (m_W) and the Z boson (m_Z).	31
9	The above table shows the values for the Fermi coupling constant (G_F), reduced Plank constant (\hbar), and the Lande factor (g).	32

10	The above table shows the masses and lifetimes of the neutrally electric charged B meson (B^0), the positively or negatively electric charged B meson (B^\pm), and the vector B meson (B^*).	32
11	The above table shows the masses and lifetimes of the neutrally electric charged D meson (D^0), the positively or negatively charged D meson (D^\pm), the positively or negatively electric charged the vector D meson ($D^{*\pm}$), and the neutrally electric charged vector D meson (D^{*0}).	32
12	The above table shows the masses of the τ particle (τ), the bottom quark (b), and the charm quark (c)	33

LIST OF FIGURES

Figure	Page	
1	(a) A particle with right-handed helicity can be seen. This can be seen as the spin vector is in the same direction as the momentum vector. (b) A particle with left-handed helicity can be seen. This can be seen as the spin vector is in the opposite direction as the momentum vector.	5
2	The above figure shows the mass differences of each generation of quarks and leptons by depicting relative spheres[13][18]	8
3	The above figure shows the Feynman diagram for the three body decay of $\bar{B} \rightarrow D^{(*)}W^{-*} (\rightarrow \ell^{-}\bar{\nu}_{\ell})$	13
4	The above figure shows the four body decay of $\bar{B} \rightarrow D^{*+} (\rightarrow D^0\pi^+) \ell^{-}\bar{\nu}_{\ell}$ complete with generalized corresponding angles and planes.)	24
5	The above figure shows the Dirac bilinear for the left handed vector current applying to the R_D ratio.	35
6	The above figure shows the Dirac bilinear for the right handed vector current applying to the R_D ratio.	36
7	The above figure shows the Dirac bilinear for the left handed scalar current applying to the R_D ratio.	37
8	The above figure shows the Dirac bilinear for the left handed tensor current applying to the R_D ratio.	38

List of Abbreviations

CI	Confidence Interval
CKM	Cabibbo-Kobayashi-Maskawa (Matrix)
CL	Confidence Limits
NP	New Physics
PDG	Particle Data Group
QED	Quantum Electrodynamics
QFT	Quantum Field Theory
SM	Standard Model

Abstract

SEARCHING FOR CLEAN OBSERVABLES IN $B \rightarrow D^* \tau^- \bar{\nu}_\tau$ DECAYS

By Michael David Williams

A Thesis submitted in partial fulfillment of the requirements for the degree of
Master of Science at Virginia Commonwealth University.

Virginia Commonwealth University, 2019.

Director: Dr. Murugeswaran Duraisamy,
Instructor, Department of Physics

In this thesis, the clean angular observables in the $\bar{B} \rightarrow D^{*+} \ell^- \bar{\nu}_\ell$ angular distribution is studied. Similar angular observables are widely studied in $B \rightarrow K^* \mu^+ \mu^-$ decays. We believed that these angular observables may have different sensitivities to different new physics structures.

INTRODUCTION

In this thesis, a theoretical study on semi-leptonic decays of the B meson of the form $B \rightarrow D\ell\nu_\ell$ and $B \rightarrow D^*\ell\nu_\ell$ is conducted. Here, B refers to the B meson, D and D^* are bound states of charm and down quarks, ℓ stands for charged leptons (electron, muon, or tau) and ν_ℓ stands for neutral leptons (electron neutrino, muon neutrino, or tau neutrino). Many physical observables have been studied in these decays with regard to the Standard Model. There are two recent experimental measurements that report a large deviation from the Standard Model predictions, one of these measurements is R_D and is the ratio between the decay rates of $B \rightarrow D\tau\nu_\tau$ and $B \rightarrow D\mu\nu_\mu$, and the other measurement is R_{D^*} , which is the ratio between the decay rates of $B \rightarrow D^*\tau\nu_\tau$ and $B \rightarrow D^*\mu\nu_\mu$. These ratios are considered to be theoretically clean observables and the reported deviations are a significant indicator for the existence of new physics.

Many theoretical papers [1][2][3] have addressed the anomalous results in R_D and R_{D^*} measurements with models other than the Standard Model. The explanations in models such as "supersymmetry" and "leptoquark" are promising. This work focuses on studying this issue in a model-independent way, such as Duraisamy et. al. has in [1][4][5][6][7][8][9][10][11][12]. The contributions to R_D and R_{D^*} from new types of interactions, as well as the full angular dependence of the semi-leptonic decays $B \rightarrow D^*\ell\nu_\ell$, were proposed in these works. A large number of observables were obtained from this angular dependence whose sensitivity to new physics effects was analyzed.

The new angular observables from $B \rightarrow D^*\ell\nu_\ell$ decays are currently being studied. These observables are expected to have low uncertainties from various theoretical inputs such as form factors. Therefore, they are expected to be theoretically clean

observables and a good place to search for physics beyond the Standard Model. In this thesis, the following tasks are focused on:

1. Theoretical background for the Standard Model and applicable theories are gone over in detail.

2. The kinematics, form factors, and angular analysis for $\bar{B} \rightarrow D^* \ell \nu_\ell$ are examined.

3. Region plots, scatter plots, and clean observables from numerical analysis are obtained for $\bar{B} \rightarrow D^* \ell \nu_\ell$. The work concludes with future work that should be done in this field.

CHAPTER 1

THEORETICAL BACKGROUND

This chapter goes through a brief overview for the motivation and the theoretical background of particle physics and the Standard Model. The chapter then discusses B mesons and some of their useful properties as it pertains to this work. The chapter concludes with a variety of fields and propagators that will be useful in finding numerical results of clean observables.

1.1 The Standard Model

The Standard Model (SM) was developed in the late 20th Century to give the best description available of the known elementary particles and fundamental forces. An elementary particle is a title given to particles that cannot be broken down further into other subgroups. The Standard Model can be categorized into four groups, these groups include quarks, leptons, gauge bosons, and scalar boson[13]. The quarks and leptons also each have respective anti-particles that are included in their categories. Along with it being a collection of previously known details of elementary particles, prior to being experimentally verified the SM was able to theoretically predict the existence of the Higgs boson, the top quark, and the tau neutrino[14].

Many predictions the SM made were eventually verified to a high precision. Although this likely seems like Einstein's elusive "Theory of Everything"[15] at first glance, this is most certainly not the case. The model does a fantastic job of describing three out of the total four fundamental forces in the universe, leaving the theory of gravitation out[16]. Along with this obvious omission there also exist some

lesser known points where the theory fails. One of these failures can be seen from observational cosmology, according to this field, the universe should contain a particle that describes the properties of dark matter[17], the SM does not account for such a particle and as such, falls short again.

1.1.1 Leptons

A lepton is an elementary particle that is a fermion and also does not undergo any strong interactions. There are three generations of leptons and for every successive generation the mass increases but the charge stays constant. Each lepton is assigned a lepton number and through a process, that number must be conserved[18][19]. Each generation includes one charged particle and one uncharged particle[16].

The first generation of leptons features the electron (charged) and the electron neutrino (uncharged). The second generation features the muon (charged) and the muon neutrino (uncharged). The third and final generation features the tau (charged) and the tau neutrino (uncharged). The electron and electron neutrino have anti-particles of positrons and electron antineutrinos, respectively. The muon and muon neutrino have anti-particles of antimuons and muon antineutrinos, respectively. Finally, the tau and tau neutrino have anti-particles of antitau and tau antineutrinos, respectively[18][19].

1.1.1.1 Spin

Because these particles are all fermions, they must obey the Pauli exclusion principle in that no two leptons of the same species can be in exactly the same state at the same time. A generalization can thus be made that a lepton can only be spin up or spin down. In short, there is no classical analog to spin, although it can be described as an intrinsic property of angular momentum and it does contribute

to the angular momentum[20]. The orbital angular momentum can be thought of as the quantum-mechanical equivalent to the classical angular momentum of orbital revolutions[21]. The spin and orbital angular momentum give a complete description of angular momentum in quantum mechanics.

1.1.1.2 Helicity

When a particle has momentum and spin in the same direction, the particle is referred to as right-handed. Alternatively, when a particle has momentum and anti-aligned spin, the particle is referred to as left-handed. This direction of a particle's spin relative to its momentum is called helicity. Mathematically, helicity can be explained by projecting the spin vector onto the momentum vector, if the resulting sign is positive then the particle is right-handed and if the resulting sign is negative then the particle is left-handed[21].

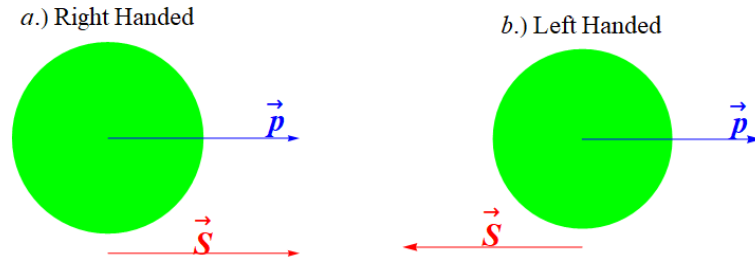


Fig. 1. (a) A particle with right-handed helicity can be seen. This can be seen as the spin vector is in the same direction as the momentum vector. (b) A particle with left-handed helicity can be seen. This can be seen as the spin vector is in the opposite direction as the momentum vector.

1.1.1.3 Parity

Employing use of a parity transformation implies the change in sign for a spatial coordinate. A parity inversion forces a situation into its mirror image and thus, a

right-handed coordinate system becomes a left-handed coordinate system under a parity transformation[22].

1.1.1.4 Anti-Leptons

For the charged particles, the respective anti-leptons flip the sign of the charge. Because each charged lepton has the same negative charge, each charged anti-lepton has the same positive charge.

1.1.2 Quarks

A quark is an elementary particle that is a fermion and also undergoes all of the fundamental interactions. Just as there are three generations of leptons, there are also three generations of quarks and for each successive generation the mass increases. Dissimilar to leptons, each different quark is given a flavor quantum number, labelled as isospin, charm, strangeness, topness, and bottomness. The anti-quarks have the opposite charge of their respective particle and each quantum number has the opposite sign.

The first generation of quarks features the up quark and the down quark where this generation is the most basic of the three. The up quark has a charge of $+2/3$ and the down quark has a charge of $-1/3$. The second generation features the charm quark and strange quark where the charm quark has charm number of $+1$ and the strange quark has a strangeness number of -1 . The charm quark has a charge of $+2/3$ and the strange quark has a charge of $-1/3$. The third and final generation features the top quark and bottom quark where the top quark has a topness number of $+1$ and the bottom quark has a bottomness number of -1 . The top quark has a charge of $+2/3$ and the bottom quark has a charge of $-1/3$ [19][21].

Quark Name	Symbol	Mass (MeV / c^2)	Q	B	S	C	\tilde{B}	T
Down	d	$m_d \approx 0.3$	$-1/3$	$1/3$	0	0	0	0
Up	u	$m_u \approx m_d$	$2/3$	$1/3$	0	0	0	0
Strange	s	$m_s \approx 0.5$	$-1/3$	$1/3$	-1	0	0	0
Charm	c	$m_c \approx 1.5$	$2/3$	$1/3$	0	1	0	0
Bottom	b	$m_b \approx 4.5$	$-1/3$	$1/3$	0	0	-1	0
Top	t	$m_t \approx 174$	$2/3$	$1/3$	0	0	0	1

Table 1. Above table shows each quark and its symbol, mass, electric charge (Q), baryon number (B), strangeness (S), charmness (C), bottomness \tilde{B} , and topness (T)[13][16]

1.1.3 Gauge/Scalar Bosons

The two varieties of elementary bosons within the SM consist of scalar bosons and gauge bosons. Bosons obey Bose-Einstein statistics, implying they have an intrinsic spin equal to an integer. The lone scalar boson within the SM is the Higgs boson, a key component of this particle is its spin equaling zero. The remaining gauge bosons all have a spin of one and are force carriers that mediate three of the four known fundamental interactions. Essentially, the SM explains forces as an exchange of matter particles and other particles.

1.1.3.1 The Electromagnetic Force

The first force to be discussed is the electromagnetic force. This force is responsible for the interaction of particles with electricity and magnetism. The boson associated with this force is the photon and is massless with an electric charge of zero. All electrically charged particles can be explained using Quantum electrodynamics (QED)[13][21].

Particle Generation	Leptons		Quarks	
First Generation	ν_e	e^- •	d •	u •
Second Generation	ν_μ	μ^- ◦	s ◦	c ◦
Third Generation	ν_τ	τ^- ◦	b ◦	t ◦

Fig. 2. The above figure shows the mass differences of each generation of quarks and leptons by depicting relative spheres[13][18]

1.1.3.2 The Weak Force

The second force with a force carrier in the SM is the weak force. This force affects all of the fermions in the SM by way of flavor changing and weak decay. There are three associated bosons for the weak interaction, they are the Z , W^- , and W^+ bosons. Although all have nonzero mass, the Z boson is the most massive of the three and is electrically neutral. The Z boson interacts with left-handed particles and antiparticles. The distinguishing difference of W^+ and W^- is their electric charge; the W^+ boson has an electric charge of positive one and the W^- boson has an electric charge of negative one. Both the W^\pm bosons act on left-handed particles and right-handed antiparticles. When the W^\pm bosons, Z boson, and the photon are grouped together, there is a theory that combines all three, known primarily as the electroweak interaction[13][21][23].

In general, the W^\pm boson in the weak interaction changes the electric charge of an elementary particle causing either a change in flavor of the quark or changing an

electron, muon, or tau into its respective neutrino. Thus, the W^\pm bosons are the mediators of neutrino absorption and emission. The Z boson will not transform an electric charge, however, instead mediates the transfer of momentum, energy, and spin as elastic scattering of neutrinos occur.

1.1.3.3 The Strong Force

The final force with a force carrier explained in the SM is the strong force. This force affects the strong interactions between quarks. The associated boson is the gluon, which is massless. Typically, quarks are described as being color charged and so are the gluons. This means that while the quark-quark interaction can be explained using gluons, the gluons themselves can also interact amongst themselves. Consequently, the gluons and the interactions are described by the theory of quantum chromodynamics (QCD). The inside of a nucleus is made up of quarks, which are in turn held together by a color force. The gluons carry a color charge and an interaction between a gluon and a quark will result in a quark that is a different color than the previous quark[21].

1.1.4 Hadrons

The SM contains information on elementary particles, although it is known that the majority of the observable universe is not referred to as each individual quark or lepton. Instead, as the elementary particles group together there are names given to the respective groupings. When two or more quarks are held together (it should be noted that there has never been experimental evidence of a single quark, they are always in a group of at least two) then the name of such a composite particle is a hadron[13].

The two main families of hadrons consist of baryons and mesons. In order to

be classified as a baryon, the constituent particle must consist of an odd number of quarks. In order to be classified as a meson, the constituent particle must be made of an even number of quarks. Because each quark is classified as a fermion, having an even number of quarks in a particle causes the spin to be a whole integer, thus making mesons be classified as bosons, similarly an odd number of quarks in a particle causes the spin to be a half integer, thus making baryons be classified as fermions[13][18].

1.1.4.1 Mesons

It is very typical for a given meson to be made up of only two quarks, although generally speaking, there will be one quark and one antiquark bound together by the strong force. There exists no meson that is stable, meaning that every single particle will decay to eventually leptons (when the meson is charged) or photons (when the meson is uncharged)[24]. An antimeson is created when the quark and antiquark pair turn to their respective antiparticles. For instance, if a meson had a quark composition $\alpha\bar{\beta}$ where α and β are given quarks, then the antimeson would be $\bar{\alpha}\beta$.

Particle	Quark Composition	Mass ($\frac{\text{MeV}}{c^2}$)	Q	S	C	\tilde{B}
π^+	$u\bar{d}$	140	+1	0	0	0
K^-	$s\bar{u}$	494	-1	-1	0	0
D^-	$d\bar{c}$	1869	-1	0	-1	0
D_s^+	$c\bar{s}$	1969	1	1	1	0
B^-	$b\bar{u}$	5279	-1	0	0	-1
Υ	$b\bar{b}$	9460	0	0	0	0

Table 2. The above table shows a few common mesons, their quark composition, mass, electric charge (Q), strangeness (S), charmness (C), and bottomness \tilde{B} [13][16][18][19][21].

1.1.5 Physics Beyond the Standard Model

As more topics are researched regarding particle physics, the SM does not change. Instead, these newfound topics are included in a category known as New Physics (NP). Current areas of NP that are being studied include finding the mass of neutrinos and explaining the asymmetric property of matter and antimatter. The SM predicts that neutrinos are massless, however this is not the case as neutrino oscillation has shown. Similarly, the SM predicts that there should be an equal amount of matter and antimatter, had this been the case then there would be no observable universe.

One specific case of the SM failing is the decay of the B meson. In recent experiments from BaBar, it has been found that existing theories are likely flawed and must be revisited[2]. This is the overarching goal of this thesis, to shed light on this difficult topic and to make predictions on how this theory can be fixed using NP. The next chapter goes in more detail on some of the issues with B mesons and why their properties are so unique[1][4][5][6][7][8][9][10][11][12][25][26][27].

1.2 B Mesons

There are four ways to create a B meson, all four ways can be seen in Table 3.

<u>Particle</u>	<u>Symbol</u>	<u>Quark Content</u>	<u>Electric Charge</u>
Positive B Meson	B^+	$u\bar{b}$	+1
Neutral B Meson	B^0	$d\bar{b}$	0
Strange B Meson	B_s^0	$s\bar{b}$	0
Charmed B Meson	B_c^+	$c\bar{b}$	+1

Table 3. The above table shows the different possible B Mesons, their quark content, and electric charges.

As stated previously, B mesons are not adequately accounted for in the SM.

Unlocking the mysteries surrounding the elusive particle is pivotal in creating NP and henceforth, particle physics as a whole. This chapter will look deeper into some of the properties of B mesons and then look at some of the repercussions of such a particle in the real world. This chapter also introduces the main topic of this thesis in the form of two processes of the B meson.

The two main processes that this thesis focuses on are $\bar{B} \rightarrow D^+ \tau^- \bar{\nu}_\tau$ and $\bar{B} \rightarrow D^{*+} \tau^- \bar{\nu}_\tau$. The D^+ and D^{*+} are a classification of D mesons, which are the lightest particle containing charm quarks. There are five ways to create a D meson, all four ways can be seen in Table 4.

<u>Particle</u>	<u>Symbol</u>	<u>Quark Content</u>	<u>Electric Charge</u>
Positive D Meson	D^+	$c\bar{d}$	+1
Neutral D Meson	D^0	$c\bar{u}$	0
Strange D Meson	D_s^+	$c\bar{s}$	+1
D Meson	D^{*+}	$c\bar{d}$	+1
D Meson	D^{*0}	$c\bar{u}$	0

Table 4. The above table shows the different possible D Mesons and their quark content and electric charges. It should be noted that while the first two and last two entries have the same quark content, the last two entries have different rest masses, total angular momenta, and the last two also have much shorter lifetimes than their counterparts.

Each of these processes can be grouped into two larger families that generalize the lepton, these families are $\bar{B} \rightarrow D^+ \ell^- \bar{\nu}_\ell$ and $\bar{B} \rightarrow D^{*+} \ell^- \bar{\nu}_\ell$ where $\ell = e, \mu$. The four body decay of the process $\bar{B} \rightarrow D^{*+} (\rightarrow D^0 \pi^+) \ell^- \bar{\nu}_\ell$ can be seen in Fig. 10[17][28].

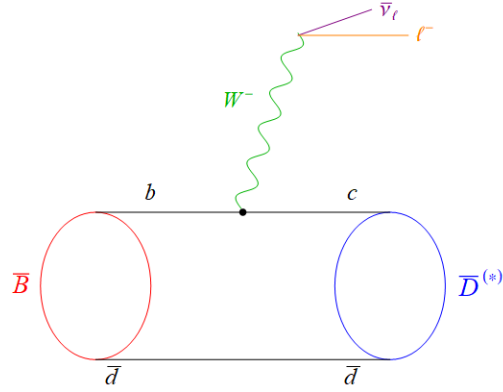


Fig. 3. The above figure shows the Feynman diagram for the three body decay of $\bar{B} \rightarrow D^{(*)}W^{-*} (\rightarrow \ell^{-}\bar{\nu}_{\ell})$.

1.2.1 CKM Mixing Matrix

Within the SM, the strength of the weak interaction in the three generations of quarks is accounted for by the Cabibbo-Kobayashi-Maskawa (CKM) matrix[29].

This process allows for the up-type quarks to be associated with the down-type quarks via the mass eigenstates. Formally, this relation is[29]

$$\begin{pmatrix} d' \\ s' \\ b' \end{pmatrix} = \begin{pmatrix} V_{ud} & V_{us} & V_{ub} \\ V_{cd} & V_{cs} & V_{cb} \\ V_{td} & V_{ts} & V_{tb} \end{pmatrix} \begin{pmatrix} d \\ s \\ b \end{pmatrix}. \quad (1.1)$$

This CKM matrix describes the probability of a transition from one quark to another quark. This methodology is very important in order to understand CP violation and this chapter goes through some of the fundamental ideas of this matrix.

1.2.2 CP Violation

Throughout particle physics, the idea of symmetry is heavily relied upon in order to give an adequate description of various phenomena. For example, earlier in Chapter One, it was said that one particle's antiparticle has opposite characteristics,

such as charge and parity. The main idea of parity symmetry is that the equations describing particle physics are invariant under mirror inversion. The main idea of charge conjugation symmetry is that a particle's antiparticle has the opposite charge of the original particle.

These two symmetries in particular can be referred to as charge conjugation (C) and parity (P) symmetries, or put together, CP symmetry.

Although not obvious, the SM does indeed account for CP violation to an extent. This occurs when a complex phase appears in the CKM matrix describing quark mixing. First consider a set of particles x and y , and their corresponding antiparticles \bar{x} and \bar{y} . Next, consider the particle process $x \rightarrow y$ and the antiparticle process $\bar{x} \rightarrow \bar{y}$ while denoting their amplitudes as M and \tilde{M} , respectively. Prior to the CP violation, these amplitude terms should have the same complex number. The magnitude and phase can be separated by[21]

$$M = |M| e^{i\theta} \tag{1.2}$$

where the phase term introduced from the CKM matrices can be denoted by $e^{i\phi}$. It should be noted here that because \tilde{M} is the complex conjugate to M then the phase is $e^{-i\phi}$. The amplitude for the particle case is[21]

$$M = |M| e^{i\theta} e^{i\phi} \tag{1.3}$$

and the amplitude for the antiparticle case is

$$\tilde{M} = |M| e^{i\theta} e^{-i\phi}. \tag{1.4}$$

These two expressions are only accounting for there being one route to go from $x \rightarrow y$ or $\bar{x} \rightarrow \bar{y}$, however. If there are unrelated intermediate states, such as $x \rightarrow$

$1 \rightarrow y$ or $x \rightarrow 2 \rightarrow y$, then the amplitudes take the form[21]

$$M = |M_1| e^{i\theta_1} e^{i\phi_1} + |M_2| e^{i\theta_2} e^{i\phi_2} \quad (1.5)$$

and

$$\tilde{M} = |M_1| e^{i\theta_1} e^{-i\phi_1} + |M_2| e^{i\theta_2} e^{-i\phi_2}. \quad (1.6)$$

The difference between the square of the amplitudes is[28][30]

$$|M|^2 - |\tilde{M}|^2 = -4 |M_1| |M_2| \sin(\theta_1 - \theta_2) \sin(\phi_1 - \phi_2). \quad (1.7)$$

Thus, a complex phase gives rise to processes that commence at different rates for particles and antiparticles, causing CP violation[28][30].

All of the interesting material concerning CP violation happens in the weak (charged current) interaction when one quark flavor changes into another quark flavor, $q \rightarrow Wq'$, even between different families.

The CP operation changes particles into anti-particles and changes the coupling constant of $q \rightarrow Wq'$ into its complex conjugate. It turns out that not all processes are invariant under the CP operation, and complex numbers can be determined.

1.2.3 Lifetimes and Cross Sections

There are three experimental probes in elementary experimental particle physics. These are bound states, decays, and scattering. In the relativistic theory, decays and scattering are well integrated into use. For a decay, it would be helpful to calculate a physical lifetime of some particle. For scattering, it would be helpful to calculate a physical cross-sectional area.

In the case of a decay, it is known that from the stationary observer, a moving particle lasts longer than a particle at rest, where this is due to time dilation. However,

this does not mean that stationary particles will all last the same amount of time, thus there appears to be an intrinsically random element within the decay. As a result or not being able to understand randomness within a particle, an observer can instead elect to measure the average lifetime of a large sample of particles. The critical parameter, as a result, is the decay rate, Γ . The physical representation of the decay rate is the probability per time that any particle will disintegrate. Over a large sample of particles, given as $N(t)$, then $N\Gamma dt$ of them would decay in the next instant dt . The number of particles can be found by

$$N(t) = N(0)e^{-\Gamma t} \quad (1.8)$$

where the mean lifetime is the reciprocal of the decay rate,

$$\tau = \frac{1}{\Gamma}. \quad (1.9)$$

However, most particles can decay by several routes. As a result, the total decay rate is the sum of the individual decay rates,

$$\Gamma_{\text{tot}} = \sum_{i=1}^n \Gamma_i \quad (1.10)$$

and the lifetime of the particle,

$$\tau = \frac{1}{\Gamma_{\text{tot}}}. \quad (1.11)$$

It would also be convenient to calculate the branching ratios, the fraction of all particles of the given type that decay by each mode. These branching ratios are determined by

$$Br_i = \frac{\Gamma_i}{\Gamma_{\text{tot}}} \quad (1.12)$$

where Br_i is the branching ratio for the i^{th} decay mode.

1.2.3.1 The Golden Rule and The Feynman Rules for a Toy Model

For both of these physical quantities discussed in the previous section, the amplitude and phase space available are the ingredients. The amplitude contains the dynamical information, and this can be found using Feynman diagrams, and as such, Feynman rules. The phase space factor contains only kinematical information, where it depends on the masses, energies, and momenta of the participating particles, thus reflecting the fact that a given process is more likely to occur the more maneuverability there is in the final state.

The transition rate for a given process is determined by the amplitude, \mathcal{M} , and the phase space according to Fermi's "Golden Rule",

$$\text{transition rate} = \frac{2\pi}{\hbar} |\mathcal{M}|^2 \times (\text{phasespace}). \quad (1.13)$$

If the assumption is made that there is a particle that decays into other particles,

$$1 \rightarrow 2 + 3 + 4 + \dots + n, \quad (1.14)$$

then the decay rate given by the formula is[13][21]

$$d\Gamma = |\mathcal{M}|^2 \frac{S}{2\hbar m_1} \left[\left(\frac{cd^3\vec{p}_2}{(2\pi)^3 2E_2} \right) \left(\frac{cd^3\vec{p}_3}{(2\pi)^3 2E_3} \right) \dots \left(\frac{cd^3\vec{p}_n}{(2\pi)^3 2E_n} \right) \right] \times \\ (2\pi)^4 \delta^4(p_1 - p_2 - p_3 - \dots - p_n) \quad (1.15)$$

with the p_n terms denoting the four momentum of the respective particle. The delta functions enforce conservation of energy and momentum. The decaying particle is presumed to be at rest. Then for each group of j identical particles in the final state, S is a product of statistical factors $\frac{1}{j!}$.

1.3 Fields and Propagators

A field is a physical quantity, represented by a number, vector, or tensor, that has a different value at every point in space. In Quantum Field Theory (QFT), an elementary excitation of a field is often referred to as the "quantum of a field". A propagator is a concept generally reserved for quantum mechanics and quantum field theory that denotes a function that specifies the probability amplitude for a particle to travel from one place to another in a given time, or to travel with a certain energy and momentum[23][31].

This chapter begins with introducing the concept of currents in the scope of particle interactions. This provides a reasonable transition to propagators and the various bilinear covariants. When discussing the fields, there is a brief aside to discuss each field's corresponding meson. The chapter then shows the usefulness of bilinear covariants in the discussion of Fermi's Golden Rule and V-A theory.

1.3.1 Charged Current and Neutral Current

As one particle interacts with another particle via the weak force, the interaction between them is typically viewed as an instantaneous result of the mediation of the weak force. In actuality, as the weak force is being mediated by either the W^\pm bosons or the Z boson, the process of such an interaction has a specific title given to it. As the W^\pm bosons are mediating the weak force, the interaction is called a "charged current" and as the Z boson is mediating the weak force, the interaction is called a "neutral current"[18][20].

In order to better explain the role of a neutral current, the characteristics of neutrinos should first be revisited. The neutrino does not interact with the electromagnetic force, because neutrinos have neutral electric charge, or the strong force,

because neutrinos are not quarks, although it does interact with the weak force. Through an interaction with a neutrino, assuming the initial and final states conserve electric charge on their own, the neutral Z boson is required. The Z boson transfers spin, energy, and momentum, but does not alter the particles' quantum numbers. Thus, through the process of a Z boson mediating the weak force, this process does exchange properties, even without an electric charge, hence the neutral title. The current that is being referred to has nothing to do with electricity, but instead referring to the movement of the Z boson[18][20][21].

A similar argument can be made for a charged current, the main difference being the transfer of electric charges and the transfer of a weak interaction charge is present in the charged current case. The W^\pm bosons do have an electric charge, hence the charged title[18][20][21].

1.3.2 Propagators

In general, there are only five possible combinations of two spinors and the gamma matrices that form Lorentz invariant currents, called "bilinear covariants". In Dirac theory, fermions are described as four-component spinor wave functions upon which 4×4 operators Γ_i apply, which are classified according to their space reflection properties.

The most general form for the interaction between a fermion and a boson is a linear combination of bilinear covariants. For an interaction corresponding to the exchange of a spin-one particle the most general form is a linear combination of vector and axial-vector bilinear covariants.

Each type of Dirac bilinear must be analyzed in order to find an adequate picture of NP. Consequently, each type of field should be analyzed in order to understand the ongoing physics.

1.3.2.1 Scalar Fields

A scalar field is a function that gives a single value of some variable for every point in space. In principle, a scalar field provides values not only on a two-dimensional surface in space but for every point in space. To represent a three dimensional scalar field, one could create a three-dimensional atmospheric volume element and color it to represent the temperature variation. The term "scalar" implies that at any point there is a number at a specified location rather than a vector[32]. Scalar Mesons

When a meson has total spin equal to zero and has even parity, then the meson is denoted as being a scalar meson. Scalar mesons can be found with a variety of masses, ranging from ($< 1\text{GeV}/c^2$)[33][34][35] to ($> 2\text{GeV}/c^2$) although the upper mass range generally contain either strange and/or bottom quarks. In this upper mass range, each have well separated masses, which provides a clear distinction and allows for easier analysis than the lower mass and intermediate mass ranges[33][34][35].

1.3.2.2 Pseudoscalar Fields

A pseudoscalar is a quantity that behaves like a scalar, except that it changes sign under a parity inversion while a true scalar does not. One of the most powerful concepts in physics is that physical laws do not change regardless of the coordinate system being used to describe said laws. However, when a coordinate system becomes inverted, a pseudoscalar changes sign. This implies that a pseudoscalar may not be the best tool to describe a physical quantity.

When a meson has total spin equal to zero and has odd parity, then the meson is denoted as being a pseudoscalar meson. Out of all the known mesons, the pseudoscalar mesons are the most well known, as the mass of many pseudoscalar mesons have been found to great precision.

1.3.2.3 Vector Fields

A vector is a quantity which has both a magnitude and a direction in space. Vectors are used to describe physical quantities such as velocity, momentum, acceleration, and force, associated with an object. However, when one tries to describe a system which consists of a large number of objects, each individual object must have a vector assigned to it.

In particle physics, when a vector boson is taken to be the quantum of a field, the field is automatically a vector field. From Table 14 it can be seen that the vector field is associated with particles that contain a spin 1. In particle physics, the gauge bosons all have a spin of one. Consequently, it can be seen that gauge bosons interact via vector fields.

When a meson has total spin equal to one and has odd parity, the meson is denoted as being a vector meson[36].

1.3.2.4 Axial Vector Fields

Also referred to as a pseudovector, an axial vector is a quantity that transforms like a vector under a proper rotation, but in three dimensions gains an additional sign flip under an improper rotation (such as a reflection). The axial vector is generally associated with the curl of a polar angle or with the cross product of two polar vectors[37]. It should be noted that while there exists a distinction between a vector and axial vector in the convention of naming, an axial vector is still a vector, but rather a different sub-group of vectors. Without a volume form there is no distinction between a vector and axial vector.

1.3.2.5 Tensor Fields

Once the idea of scalar fields and vector fields are understood, the generalization to tensor fields is simple. Instead of assigning a scalar or vector to each point in space, as scalar fields and vector fields do, respectively, a tensor field assigns a tensor.

Type	S	L	P	J	J^P
Scalar Meson	1	1	+	0	0^+
Pseudoscalar Meson	0	0	-	0	0^-
Vector Meson	1	0, 2	-	1	1^-
Axial Vector Meson	1	1	+	1	1^+
Tensor Meson	1	1, 3	+	2	2^+

Table 5. The above table denotes the types of mesons and the corresponding value of their spin (S), orbital angular momentum (L), parity transformation (P), total angular momentum (J), and the combination of the total angular momentum with the parity transformation (J^P).

CHAPTER 2

FORMALISM OF $\bar{B} \rightarrow D^{(*)} \ell^{-} \nu_{\ell}$

In order to examine the angular distribution from the $B \rightarrow D^{(*)} \ell^{-} \nu_{\ell}$ decay, the Effective Hamiltonian must be found. The relevant kinematics can be seen throughout.

In the presence of NP, the Effective Hamiltonian for the quark level transition $b \rightarrow c \ell^{-} \bar{\nu}_{\ell}$, where $\ell = e, \mu, \tau$, can be written in the form[1]

$$\begin{aligned}
 \mathcal{H}_{\text{eff}} = & \frac{4G_F V_{cb}}{\sqrt{2}} [(1 + V_L) [\bar{c} \gamma_{\mu} P_L b] [\bar{\ell} \gamma^{\mu} P_L \nu_{\ell}] + \\
 & V_R [\bar{c} \gamma^{\mu} P_R b] [\bar{\ell} \gamma_{\mu} P_L \nu_{\ell}] + S_L [\bar{c} P_L b] [\bar{\ell} P_L \nu_{\ell}] + \\
 & S_R [\bar{c} P_R b] [\bar{\ell} P_L \nu_{\ell}] + T_L [\bar{c} \sigma^{\mu\nu} P_L b] [\bar{\ell} \sigma_{\mu\nu} P_L \nu_{\ell}]
 \end{aligned} \tag{2.1}$$

where G_F is the Fermi coupling constant, V_{cb} is the CKM matrix element, $P_L = (1 - \gamma_5)/2$ (projector for negative chiralities), $P_R = (1 + \gamma_5)/2$ (projector for positive chiralities), and $\sigma_{\mu\nu} = i [\gamma_{\mu}, \gamma_{\nu}]/2$. It is also assumed that the chirality of the neutrino is always left. The effective Hamiltonian for the Standard Model assumes that $V_L = V_R = S_L = S_R = T_L = 0$ [1].

2.1 Discussion of $B \rightarrow D\ell\nu_\ell$

The angular distribution for the decay $\bar{B} \rightarrow D^+\tau^-\bar{\nu}_\tau$, with NP operators, can be written as [1]

$$\frac{d\Gamma^D}{dq^2 d\cos(\theta_\ell)} = 2N_D |p_D| \left[|H_0|^2 \sin^2(\theta_\ell) + \frac{m_\ell^2}{q^2} (H_0 \cos(\theta_\ell) - H_{tS})^2 + s \left(\left(\left(1 + \frac{m_\ell^2}{q^2} \right) + \left(1 - \frac{m_\ell^2}{q^2} \right) \cos(2\theta_\ell) \right) |H_T|^2 - \frac{m_\ell}{\sqrt{q^2}} \text{Re}[H_T (H_0^* - H_{tS}^* \cos(\theta_\ell))] \right) \right] \quad (2.2)$$

where the helicity amplitudes are given in [1].

2.2 Discussion of $B \rightarrow D^*\ell\nu_\ell$

The complete three-angle distribution for the decay $\bar{B} \rightarrow D^*\ell\bar{\nu}_\ell$ can be found in [1]. In the presence of NP, the distribution can be expressed in terms of four kinematic variables q^2 , two polar angles θ_ℓ , θ_{D^*} , and the azimuthal angle χ . The angle θ_ℓ is the polar angle between the charged lepton and the direction opposite to the D^* meson in the $(\ell\nu_\ell)$ rest frame. The angle θ_{D^*} is the polar angle between the D meson and the direction of the D^* meson in the $(D\pi)$ rest frame. The angle χ is the azimuthal angle between the two decay planes spanned by the 3-momenta of the $(D\pi)$ and $(\ell\nu_\ell)$ systems. These angles are described in Fig. 4[1].

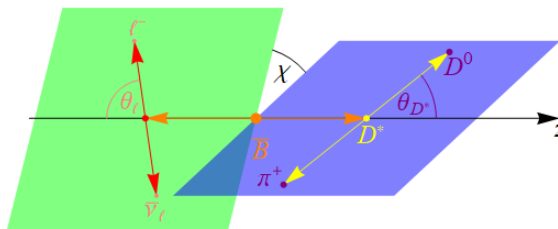


Fig. 4. The above figure shows the four body decay of $\bar{B} \rightarrow D^{*+} (\rightarrow D^0\pi^+) \ell^-\bar{\nu}_\ell$ complete with generalized corresponding angles and planes.)

2.2.1 Form Factors

A form factor is a way to explain particular properties of a particle interaction without giving every single detail of the physics. These terms are thus a way to examine the specific areas of interest while maintaining the integrity of the physical phenomena in question. The form factors are modified to fit experimental results so that future experiments can potentially benefit from newfound knowledge. When form factors do not require an experimental fit, but rather rely purely on symmetry, the form factors are often given the title of "clean observables". Clean observables are preferred over experimental fits because experimental results rely on imperfect results that may improve as technology improves.

From Melikhov, et. al. [38], it can be seen that the long distance contribution to meson decays is contained in the relativistic invariant transition form factors of the vector, axial-vector, and tensor currents. The amplitudes of the $M_1 \rightarrow M_2$ transition induced by the weak $q_2 \rightarrow q_1$ quark transition through the vector

$$V_\mu = \bar{q}_1 \gamma_\mu q_2, \tag{2.3}$$

axial vector

$$A_\mu = \bar{q}_1 \gamma_\mu \gamma^5 q_2, \tag{2.4}$$

tensor

$$T_{\mu\nu} = \bar{q}_1 \sigma_{\mu\nu} q_2, \tag{2.5}$$

and pseudotensor

$$T_{\mu\nu}^5 = \bar{q}_1 \sigma_{\mu\nu} \gamma_5 q_2 \tag{2.6}$$

currents, have the covariant structures[38]

$$\langle P(M_2, p_2) | V_\mu(0) | P(M_1, p_1) \rangle = f_+(q^2) P_\mu + f_-(q^2) q_\mu, \quad (2.7)$$

$$\langle V(M_2, p_2, \epsilon) | V_\mu(0) | P(M_1, p_1) \rangle = 2g(q^2) \epsilon_{\mu\nu\alpha\beta} \epsilon^{*\nu} p_1^\alpha p_2^\beta, \quad (2.8)$$

$$\langle V(M_2, p_2, \epsilon) | A_\mu(0) | P(M_1, p_1) \rangle = i \epsilon^{*\alpha} [f(q^2) g_{\mu\alpha} + a_+(q^2) p_{1\alpha} P_\mu + a_-(q^2) p_{1\alpha} q_\mu], \quad (2.9)$$

$$\langle P(M_2, p_2) | T_{\mu\nu}(0) | P(M_1, p_1) \rangle = -2i s(q^2) (p_{1\mu} p_{2\nu} - p_{1\nu} p_{2\mu}), \quad (2.10)$$

$$\begin{aligned} \langle V(M_2, p_2, \epsilon) | T_{\mu\nu}(0) | P(M_1, p_1) \rangle = i \epsilon^{*\alpha} [g_+(q^2) \epsilon_{\mu\nu\alpha\beta} P^\beta + \\ g_-(q^2) \epsilon_{\mu\nu\alpha\beta} q^\beta + g_0(q^2) p_{1\alpha} \epsilon_{\mu\nu\beta\gamma} p_1^\beta p_2^\gamma], \end{aligned} \quad (2.11)$$

where $q = p_1 - p_2$ and $P = p_1 + p_2$. The double spectral densities of the form factors are obtained by calculating the relevant traces and isolating the Lorentz structures depending on \tilde{p}_1 and \tilde{p}_2 . These invariant factors \tilde{f} account for the two-particle singularities in the Feynman graph.

Following the guideline set forth by Melikhov, et. al. [38], the connection between known masses and form factors F_+ , F_0 , f_T , V , A_0 , A_1 , A_2 , T_1 , T_2 , and T_3 can be determined as linear combinations of the form factors found from the covariant

structures above. The linear combinations of the form factors go as

$$F_+ = f_+, \quad (2.12)$$

$$F_0 = f_+ + \frac{q^2}{P_q} f_-, \quad (2.13)$$

$$F_T = -(M_1 + M_2) s, \quad (2.14)$$

$$V = (M_1 + M_2) g, \quad (2.15)$$

$$A_1 = \frac{1}{M_1 + M_2} f, \quad (2.16)$$

$$A_2 = -(M_1 + M_2) a_+, \quad (2.17)$$

$$A_0 = \frac{1}{2M_2} (f + q^2 a_- + P_q a_+), \quad (2.18)$$

$$T_1 = -g_+, \quad (2.19)$$

$$T_2 = -g_+ - \frac{q^2}{P_q} g_-, \quad (2.20)$$

$$T_3 = g_- - \frac{P_q}{2} g_0. \quad (2.21)$$

There exists a parameterizing fit function that interpolates the results of the calculation of the form factors F_+ , F_T , V , T_1 , and A_0 that goes as

$$f(q^2) = \frac{f(0)}{\left(1 - \frac{q^2}{M^2}\right) \left(1 - \frac{q^2}{(\alpha M)^2}\right)}. \quad (2.22)$$

To achieve the accuracy for the form factors at less than one percent, then the fit function takes the form

$$f(q^2) = \frac{f(0)}{\left(1 - \frac{q^2}{M^2}\right) \left(1 - \frac{\sigma_1 q^2}{M^2} + \frac{\sigma_2 q^4}{M^4}\right)}. \quad (2.23)$$

Then for the form factors F_0 , A_1 , A_2 , T_2 , and T_3 , the contributing resonances lie farther away from the physical decay region and the effect of any particular resonance is smeared out. For these form factors, the interpolation function is

$$f(q^2) = \frac{f(0)}{1 - \frac{\sigma_1 q^2}{M_V^2} + \frac{\sigma_2 q^4}{M_V^4}}. \quad (2.24)$$

Finally, using the same parameters as Melikhov, et. al. [38], the form factors for the transition $B \rightarrow D$ can be seen in Table 7.

Then using the same parameters as Melikhov, et. al. [38], the form factors for the transition $B \rightarrow D^*$ can be seen in Table 8.

	F_+	F_0	F_T
$f(\mathbf{0})$	0.67	0.67	0.69
σ_1	0.57	0.78	0.56

Table 6. The above table shows the values of the form factors during the transition $B \rightarrow D$.

	V	A_0	A_1	A_2	T_1	T_2	T_3
$f(\mathbf{0})$	0.76	0.69	0.66	0.62	0.68	0.68	0.33
σ_1	0.57	0.58	0.78	1.40	0.57	0.64	1.46
σ_2				0.41			

Table 7. The above table shows the values of the form factors during the transition $B \rightarrow D^*$.

2.3 Angular Observables in $\bar{B} \rightarrow D^* \ell \nu_\ell$

One of the most important aspects of analysis in determining the clean observables from $\bar{B} \rightarrow D^* \ell \nu_\ell$ is examining the angular distribution from the decay process. The parameters can be determined and then symmetry can be exploited to find clean observables[39]. This is very important for the future of such studies in B meson decays[40][41][42].

The angular distribution of $\bar{B} \rightarrow D^*(\rightarrow D\pi)\ell^-\bar{\nu}_\ell$ can be found from [1] as

$$\begin{aligned}
\frac{d\Gamma}{dq^2 d\cos(\theta_\ell) d\cos(\theta_{D^*}) d\chi} &= \frac{9}{32\pi} N_F \left\{ \cos^2(\theta_{D^*}) (J_1^0 + \right. \\
& J_2^0 \cos(2\theta_\ell) + J_3^0 \cos(\theta_\ell)) + \\
& \sin^2(\theta_{D^*}) (J_1^T + J_2^T \cos(2\theta_\ell) + J_3^T \cos(\theta_\ell)) + \\
& J_4^T \sin^2(\theta_{D^*}) \sin^2(\theta_\ell) \cos(2\chi) + J_1^{0T} \sin(2\theta_{D^*}) \sin(2\theta_\ell) \cos(\chi) + \\
& J_2^{0T} \sin(2\theta_{D^*}) \sin(\theta_\ell) \cos(\chi) + J_5^T \sin^2(\theta_{D^*}) \sin^2(\theta_\ell) \sin(2\chi) + \\
& \left. J_3^{0T} \sin(2\theta_{D^*}) \sin(\theta_\ell) \sin(\chi) + J_4^{0T} \sin(2\theta_{D^*}) \sin(2\theta_\ell) \sin(\chi) \right\} \quad (2.25)
\end{aligned}$$

where the quantity N_F is

$$N_F = \left[\frac{G_F^2 |p_{D^*}| |V_{cb}|^2 q^2}{3 (2^6) \pi^3 m_B^2} \left(1 - \frac{m_\ell^2}{q^2} \right)^2 \text{Br}(D^* \rightarrow D \pi) \right]. \quad (2.26)$$

The angular coefficients can be found in [1].

The differential decay rate can be obtained after performing integration over all the angles

$$\frac{d\Gamma}{dq^2} = \frac{3N_F}{4} (A_L + A_T). \quad (2.27)$$

The D^* meson's longitudinal and transverse polarization amplitudes are

$$A_L = \left(V_1^0 - \frac{1}{3} V_2^0 \right) \quad (2.28)$$

and

$$A_T = 2 \left(V_1^T - \frac{1}{3} V_2^T \right), \quad (2.29)$$

respectively.

CHAPTER 3

NUMERICAL ANALYSIS

Thus far in this work, background information and the formalism for $\bar{B} \rightarrow D^{(*)} \ell \nu_\ell$ has been discussed, along with relevant form factors and angular analysis. It is time to put some of these values to use, just as Duraisamy et. al. did in [1]. This chapter begins with the discussion of region plots, where the allowed region for complex coupling of varying currents are found at different confidence levels. The chapter then discusses scatter plots from the relevant currents. The chapter uses these tools to relate Sec. 2.3 and the desired value for the clean observables. The chapter concludes with a summary and discussion on future work. The results here depend on the results from R_D and R_{D^*} .

The results found throughout are many constants that are found from Tanabashi, et. al. [43] and the entire Particle Data Group (PDG). The values for the mass of the relevant gauge bosons given in [43] can be seen in Table 8. The values for three

m_W (GeV)	m_Z (GeV)
80.379 ± 0.012	91.1876 ± 0.0021

Table 8. The above table shows the masses of the W boson (m_W) and the Z boson (m_Z).

relevant physical constants can be seen in Table 9. It should be noted that g can be found as

$$g = \sqrt{\frac{8m_W^2 G_F}{\sqrt{2}}}. \quad (3.1)$$

G_F (GeV ⁻²)	\hbar (GeV ps)	g
1.1663787×10^{-5}	$6.582119514 \times 10^{-13}$	0.652905

Table 9. The above table shows the values for the Fermi coupling constant (G_F), reduced Planck constant (\hbar), and the Lande factor (g).

The values for the relevant bottom meson masses and lifetimes can be seen in Table 10. It should be noted that for the vector B meson in Table 11, the neutrally,

Meson	Mass (GeV)	Lifetime (ps)
B^0	5.27963 ± 0.00015	1.520 ± 0.004
B^\pm	5.27932 ± 0.00014	1.638 ± 0.004
B^*	5.32465 ± 0.00025	1.520 ± 0.004

Table 10. The above table shows the masses and lifetimes of the neutrally electric charged B meson (B^0), the positively or negatively electric charged B meson (B^\pm), and the vector B meson (B^*).

positively, and negatively electric charged vector B mesons yield the same mass to six significant figures. The values for the relevant charmed meson masses and lifetimes can be seen in Table 11. Finally, the values for the relevant lepton and quark masses

Meson	Mass (GeV)	Lifetime (ps)
D^0	1.86483 ± 0.00005	0.4101 ± 0.0015
D^\pm	1.86965 ± 0.00005	0.1040 ± 0.007
$D^{*\pm}$	2.01026 ± 0.00005	$(7.89 \pm 0.17) \times 10^{-9}$
D^{*0}	2.00685 ± 0.00005	$> 3.1 \times 10^{-10}$

Table 11. The above table shows the masses and lifetimes of the neutrally electric charged D meson (D^0), the positively or negatively charged D meson (D^\pm), the positively or negatively electric charged the vector D meson ($D^{*\pm}$), and the neutrally electric charged vector D meson (D^{*0}).

can be seen in Table 12.

Particle	Average Mass (GeV)
τ (Lepton)	1.776860 ± 1.20
b (Quark)	4.18 ± 0.04
c (Quark)	1.275 ± 0.035

Table 12. The above table shows the masses of the τ particle (τ), the bottom quark (b), and the charm quark (c)

3.1 Region Plots

It is important to determine what values can be expected from the model to gain insight into what the actual measured data may be. This is the premise behind Confidence Intervals (CI). In other words, the CI indicates a range of values that is likely to encompass the true value. The range that constitutes the CI contain an upper and lower limit that are called Confidence Limits (CL). If CIs are created using a given CL from an infinite number of independent sample statistics, the proportion of those intervals that contain the true value of the parameter will be equal to the CL[44].

One method in particle physics that employs use of CIs is R_D/R_{D^*} anomalies[3]. Writing out $R_{D^{(*)}}$ is done by creating a ratio of branching ratios for one particular decay over the branching ratio for general decays of the same form,

$$R_{D^{(*)}} = \frac{\text{Br}(B \rightarrow D^{(*)}\tau^-\bar{\nu}_\tau)}{\text{Br}(B \rightarrow D^{(*)}\ell^-\bar{\nu}_\ell)}. \quad (3.2)$$

The predictions made by the SM are very different than what is found in experimental data. This points to the possibility of NP and should be investigated[3]. The

upper CL for R_{D^*} is dependent on the standard deviation σ and is found by

$$R_{D^{(*)}(UB)}(\sigma) = R_{D^*} + d R_{D^*} \sigma \quad (3.3)$$

where d denotes a change, or more appropriately, an error. The lower CL for $R_{D^{(*)}}$ is then

$$R_{D^{(*)}(LB)}(\sigma) = R_{D^*} - d R_{D^*} \sigma. \quad (3.4)$$

The upper and lower CLs can also be found for R_D , they are

$$R_{D(UB)}(\sigma) = R_D + d R_D \sigma \quad (3.5)$$

and

$$R_{D(LB)}(\sigma) = R_D - d R_D \sigma, \quad (3.6)$$

respectively. The physical meaning of this σ is very important, while it does represent a standard deviation, it is generally accepted that all data lies within three standard deviations of the mean. However, in particle physics, in order to qualify as a discovery, there must be a five sigma confidence level[44].

From Hirose and the Belle Collaboration[45] the measurement of the upper and lower bounds for $R_{D^{(*)}}$ is

$$R_{D^*} = 0.316 \pm 0.019 \quad (3.7)$$

and the measurement of the upper and lower bounds for R_D is

$$R_D = 0.397 \pm 0.049. \quad (3.8)$$

The experimental results of R_{D^*} in Eq. (3.7) and R_D in Eq. (3.8) are used to constrain different NP couplings in the Hamiltonian in Eq. (2.1).

When the Dirac bilinear for the left handed vector current is plotted in a region that bounds 2σ and 3σ , the result can be seen in Fig. 5. When the Dirac bilinear

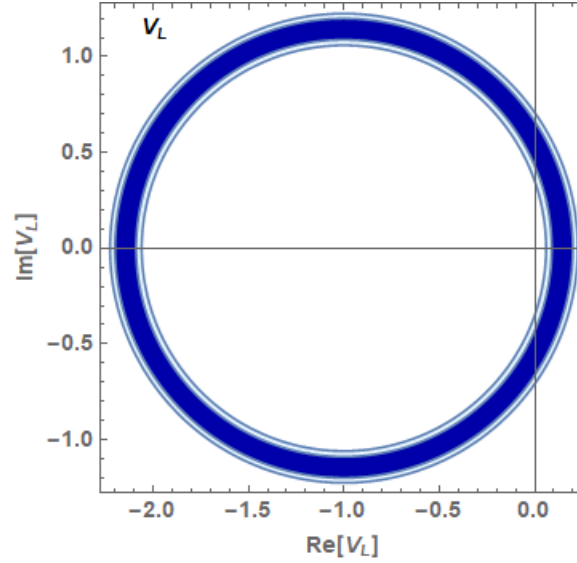


Fig. 5. The above figure shows the Dirac bilinear for the left handed vector current applying to the R_D ratio.

for the right handed vector current is plotted in a region that bounds 2σ and 3σ , the result can be seen in Fig. 6. When the Dirac bilinear for the left handed scalar current is plotted in a region that bounds 2σ and 3σ , the result can be seen in Fig. 7. Finally, When the Dirac bilinear for the left handed tensor current is plotted in a region that bounds 2σ and 3σ , the result can be seen in Fig. 8.

3.2 Moving Forward

With the main contributions from [1][46], this section allows for the numerical findings of clean observables. These values do not rely on models or form factors, and are instead purely based on symmetry.

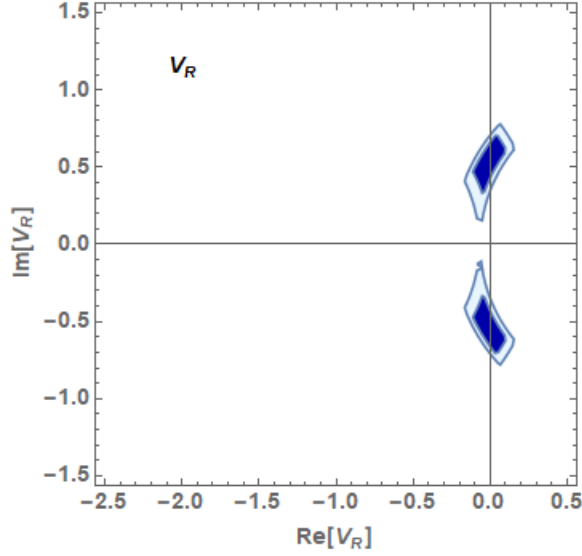


Fig. 6. The above figure shows the Dirac bilinear for the right handed vector current applying to the R_D ratio.

3.2.1 Clean Observables

The clean angular observables that are studied in this thesis are P'_4 , P'_5 , and P'_6 . Then, the connection between the angular coefficients V and the clean observables P'_4 , P'_5 , and P'_6 are [39]

$$P'_4 = P_4 \sqrt{1 - P_1} = \frac{J_{10T}}{\sqrt{-J_{20}J_{2T}}}, \quad (3.9)$$

$$P'_5 = P_5 \sqrt{1 + P_1} = \frac{J_{20T}}{2\sqrt{-J_{20}J_{2T}}}, \quad (3.10)$$

and

$$P'_6 = P_6 \sqrt{1 - P_1} = -\frac{J_{30T}}{2\sqrt{-J_{20}J_{2T}}}. \quad (3.11)$$

These angular observables are extensively studied in $B \rightarrow K^* \mu^+ \mu^-$. The observables are expected to have low uncertainties from various theoretical inputs, such as

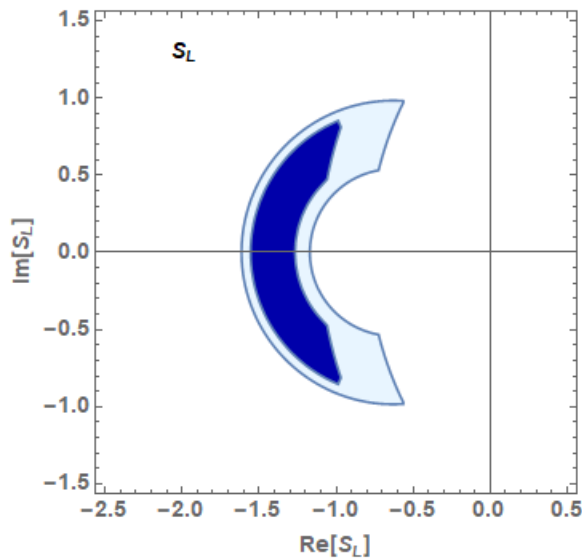


Fig. 7. The above figure shows the Dirac bilinear for the left handed scalar current applying to the R_D ratio.

form factors. Hence, they are expected to be theoretically clean observables and a good place to search for NP. These observables depend on NP couplings, there we expect they may have different sensitivities to different NP structures. This analysis will be done in the future.

3.3 Discussion

In this thesis, theoretical background material of the Standard Model, B mesons and relevant properties, and fields and propagators were summarized in chapter one. In chapter two, the formalism of $\bar{B} \rightarrow D^+ \tau^- \bar{\nu}_\tau$ was summarized, along with kinematics, angular distributions, and form factors. The chapter concluded with the discussion of $\bar{B} \rightarrow K^* \mu^+ \mu^-$ and how the angular analysis done here can be used to find desired clean observables, which are dependent on the results from R_D and R_{D^*} .

The clean observables allow insight into physics beyond the Standard Model. Although this is one small piece to the puzzle, the material is important for further

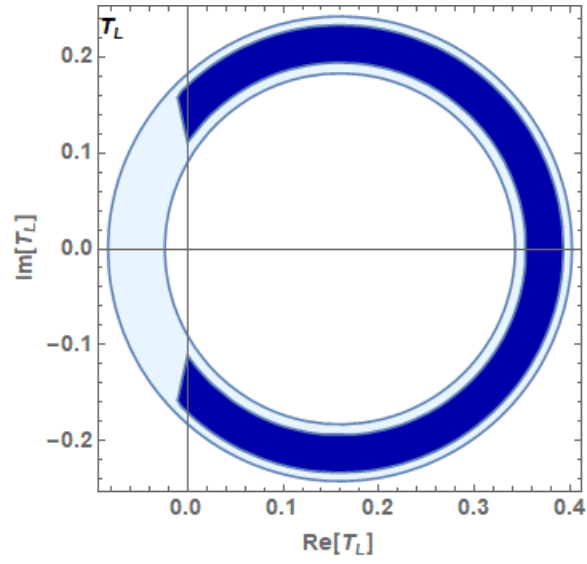


Fig. 8. The above figure shows the Dirac bilinear for the left handed tensor current applying to the R_D ratio.

investigations.

BIBLIOGRAPHY

- [1] Murugeswaran Duraisamy. “Azimuthal $B \rightarrow D^* \tau^- \bar{\nu}_\tau$ Angular Distribution with Tensor Operators”. In: *Physical Review D* 90.7 (2014).
- [2] The BaBar Collaboration. “Evidence for an excess of $\bar{B} \rightarrow D^{(*)} \tau^- \bar{\nu}_\tau$ Decays”. In: *Physical Review Letters* 109.10 (2012).
- [3] Debjyoti Bardhan. “A Closer Look at the R_D and R_{D^*} Anomalies”. In: *Journal of High Energy Physics* 2017.1 (2017).
- [4] Murugeswaran Duraisamy. “Rare Semileptonic $B \rightarrow K(\pi) \ell_i^- \ell_j^+$ Decay in a Vector Leptoquark Model”. In: *Physical Review D* 95.3 (2017).
- [5] Alakabha Datta. “Explaining The $B \rightarrow K^* \mu^+ \mu^-$ Data with Scalar Interactions”. In: *Physical Review D* 89.7 (2014).
- [6] Bhubanjoyti Bhattacharya. “Searching for New Physics with $\bar{b} \rightarrow \bar{s} B_s^0 \rightarrow V_1 V_2$ Penguin Decays”. In: *Physical Review D* 88.1 (2013).
- [7] Murugeswaran Duraisamy. “The Full $B \rightarrow D^* \tau^- \bar{\nu}_\tau$ Angular Distribution and CP Violating Triple Products”. In: *Journal of High Energy Physics* 2013.9 (2013).
- [8] Dris Boubaa. “Predictions for $B \rightarrow \tau \bar{\mu} + \mu \bar{\tau}$ ”. In: *International Journal of Modern Physics A* 28.31 (2013).
- [9] Alakabha Datta. “New Physics in $\bar{b} \rightarrow \bar{s}$ Transitions and the $B_{ds^0} \rightarrow V_1 V_2$ Angular Analysis”. In: *Physical Review D* 86.7 (2012).
- [10] Alakabha Datta. “Diagnosing New Physics in $\bar{b} \rightarrow c \tau \nu_\tau$ Decays in the Light of the Recent BaBar Result”. In: (), pp. 1–24.

- [11] Ashutosh Kumar Alok. “New Physics in $b \rightarrow s\mu^+\mu^-$: CP-Violating Observables”. In: *Journal of High Energy Physics* 2011.11 (2011).
- [12] Alakabha Datta. “Searching for New Physics with B Decay Fake Triple Products”. In: *Journal of High Energy Physics* 2011.11 (2011).
- [13] David Jeffrey Griffiths. *Introduction to Elementary Particles*. 1st ed. Wiley-VCH Verlag, 2014.
- [14] R. Rosenfeld. “Physics Beyond the Standard Model”. In: *CERN Yellow Pages* 5 (2016).
- [15] Zhiliang Cao. “Theory of Everything”. In: *Frontiers of Astronomy, Astrophysics, and Cosmology* 1.1 (2015), pp. 31–36.
- [16] B. R. Martin. *Particle Physics*. 1st ed. Wiley Sons, 2017.
- [17] Ben Gripaios. “Lectures on Physics Beyond the Standard Model”. In: (2015).
- [18] Kerson Huang. *Quarks, Leptons Gauge Fields*. 1st ed. World Scientific, 1992.
- [19] K. M. Case. “Reformulation of the Majorana Theory of the Neutrino”. In: *Physical Review* 107.1 (1957), pp. 307–316.
- [20] Franz Gross. *Relativistic Quantum Mechanics and Field Theory*. 1st ed. Wiley-VCH Verlag, 2006.
- [21] Michael E. Peskin. *An Introduction to Quantum Field Theory*. 1st ed. College Press, 1998.
- [22] P. A. M. Dirac. *Lectures on Quantum Mechanics and Relativistic Field Theory*. 1st ed. Martino Fine Books, 2012.
- [23] G. Rajasekaran. “Fermi and the Theory of Weak Interactions”. In: *Institute of Mathematica Sciences* 1.1 (2014).

- [24] Dean Lee. “Mesons with a Light Quark-Antiquark Pair and the Bethe-Salpeter Equation”. In: (1994).
- [25] Ashutosh Kumar Alok. “New Physics in $b \rightarrow s\mu^+\mu^-$: CP-Conserving Observables”. In: *Journal of High Energy Physics* 2011.11 (2011).
- [26] Cheng-Wei Chiang. “New Physics in $B_s^0 \rightarrow J/\Psi\phi$: a General Analysis”. In: *Journal of High Energy Physics* 2010.4 (2010).
- [27] Cheng-Wei Chiang. “Angular Analysis and CP Violation Studies in B Decays at CMS”. In: *Journal of Physics: Conference Series* 556 (2014).
- [28] A. J. Bevan. “The Physics of the B Factories”. In: *The European Physical Journal C* 74.11 (2014), pp. 1–3026.
- [29] Sebastien Descotes-Genon. “The CKM Parameters”. In: *Annual Review of Nuclear and Particle Science* 67 (2017), pp. 97–127.
- [30] Kenkichi Miyabayashi. “Time-Dependent CP Violation and Mixing at B Factories”. In: *Acta Physica Polonica B* 43.7 (2012), pp. 1553–1560.
- [31] Yorikiyo Nagashima. *Elementary Particle Physics*. 1st ed. Wiley-VCH Verlag, 2013.
- [32] G. H. Weber. “Exploring Scalar Fields Using Critical Isovalues”. In: *Institute of Electrical and Electronics Engineers* (2002), pp. 171–178.
- [33] H. O. Cohn. “Search for a Neutral Scalar Meson”. In: *Physical Review Letters* 15.23 (1965), pp. 906–908.
- [34] Tadayuki Teshima. “Effects to Scalar Meson Decays of Strong Mixing Between Low and High Mass Scalar Mesons”. In: *AIP Conference Proceedings* 717 (2004), pp. 150–154.

- [35] N.N. Achasov. “The Problem of Scalar Mesons”. In: *Soviet Physics Uspekhi* 161.27 (1984), pp. 161–180.
- [36] E. Kyriakopoulos. “Vector Meson Interaction Hamiltonian”. In: *Physical Review Journals Archive* 183.5 (1969), pp. 1318–1323.
- [37] I. Brevik. “Polar and Axial Vectors in Electrodynamics”. In: *American Journal of Physics* 40.4 (1972), pp. 550–552.
- [38] D. Melikhov. “Weak Form Factors for Heavy Meson Decays: An Update”. In: *Physical Review D* 62.1 (2000).
- [39] Linwei Li. “Rare B Decays at CMS”. In: *The Conference on Large Hadron Collider Physics* 5 (2017).
- [40] Aqsa Nasrullah. “Analysis of Angular Observables of $\Lambda_b \rightarrow \Lambda (\rightarrow p\pi) \mu^+ \mu^-$ Decay in Standard and Z' Models”. In: *Progress of Theoretical and Experimental Physics* 2018.4 (2018).
- [41] Shibasis Roy. “Lepton Mass Effects and Angular Observables in $\Lambda_b \rightarrow \Lambda (\rightarrow p\pi) \ell^+ \ell^-$ ”. In: *Physical Review D* 96.11 (2017).
- [42] Svetlana Fajfer. “Testing Spin-2 Mediator by Angular Observables in $b \rightarrow s\mu^+ \mu^-$ ”. In: *Physical Review D* 97.9 (2018).
- [43] M. Tanabashi. “2018 Review of Particle Physics”. In: *Physical Review D* 98.1 (2018).
- [44] Michael Plischke. *Equilibrium Statistical Physics*. 3rd ed. World Scientific, 2006.
- [45] Belle Collaboration. “Measurement of the τ Lepton Polarization and $R(D^*)$ in the Decay $\bar{B} \rightarrow D^* \tau^- \bar{\nu}_\tau$ with One-Prong Hadronic τ Decays at Belle”. In: *Physical Review D* 97.1 (2018).

- [46] Joaquim Matias. “Complete Anatomy of $\bar{B}_d \rightarrow \bar{K}^{*0} \ell^+ \ell^-$ and its Angular Distribution”. In: *Journal of High Energy Physics* 104.4 (2012).
- [47] Ernest S. Abers. *Quantum Mechanics*. 1st ed. Pearson Education, 2004.
- [48] Frank Wilczek. “QCD Made Simple”. In: *Physics Today* 53.8 (2000), pp. 22–28.
- [49] Michael H. Seymour. “Quantum ChromoDynamics”. In: *Latin America School of High Energy Physics* 1.1 (2009).
- [50] V. Shtabovenko. “New Developments in FeynCalc 9.0”. In: *Computer Physics Communications* 207.1 (2016), pp. 432–444.
- [51] R Mertig. “Feyn Calc - Computer-Algebraic Calculation of Feynman Amplitudes”. In: *Computer Physics Communications* 64.3 (1991), pp. 345–359.
- [52] Blazenka Melic. “LCSR Analysis of Exclusive Two-Body B Decay into Charmonium”. In: *Physics Letters B* 591.1-2 (2004), pp. 91–96.
- [53] Thomas Hahn. “Generating Feynman Diagrams and Amplitudes with FeynArts 3”. In: *Computer Physics Communications* 140.3 (2001), pp. 418–431.
- [54] J. Kublbeck. “Feyn Arts - Computer Algebraic Generation of Feynman Graphs and Amplitudes”. In: *Computer Physics Communications* 60.2 (1990), pp. 165–180.
- [55] A. V. Bednyakov. “The Mathematica Package for Calculation of One-Loop Penguins in FCNC Processes”. In: *International Journal of Modern Physics C* 26.4 (2013).
- [56] C.P. Burgess. “Model-Independent Global Constraints on New Physics”. In: *Physical Review D* 49.11 (1994), pp. 6115–6147.
- [57] Andrey G. Grozin. *Heavy Quark Effective Theory*. 1st ed. Springer, 2004.

- [58] Matthias Neubert. “Heavy-Quark Effective Theory”. In: *Lectures at the 34th International School of Subnuclear Physics* 1.1 (1996), pp. 1–45.
- [59] A. Ali. “Helicity Analysis of the Decays $B \rightarrow K^* \ell^+ \ell^-$ and $B \rightarrow \rho \ell \nu_\ell$ in the Large Energy Effective Theory”. In: *The European Physical Journal C* 25.3 (2002), pp. 583–601.
- [60] Ugo Aglietti. “Factorization and Effective Field Theories”. In: *Physics Letters B* 431.1-2 (1998).
- [61] ATLAS Collaboration. “Searches for Third-Generation Scalar Leptoquarks in $\sqrt{s} = 13\text{TeV}$ pp Collisions with the ATLAS Detector”. In: *Journal of High Energy Physics* (2019).
- [62] K.A. Olive. “Supersymmetry (Theory)”. In: *Particle Data Group* (2014), pp. 1–55.
- [63] M Dobre. “ATLAS Detector Upgrade Prospects”. In: *Journal of Physics: Conference Series* 798 (2017), pp. 1–8.
- [64] ATLAS Collaboration. “Prospects for a Search for Direct stau Production in Events with at Least Two Hadronic taus and Missing Transverse Momentum at the High Luminosity LHC with the ATLAS Detector”. In: *ATLAS Physics Collaboration* (2016).
- [65] Achintya Rao. “The Hunt for Leptoquarks is on”. In: *CERN’s Courier September 2018* (2018).
- [66] Howard Georgi. “Effective Field Theory”. In: *Annual Review of Nuclear and Particle Science* 43 (1993), pp. 209–252.
- [67] Sung-Sik Lee. “Low-Energy Effective Theory of Fermi Surface Coupled with $U(1)$ Gauge Field in $2 + 1$ Dimensions”. In: *Physical Review B* 80.16 (2009).

- [68] A. S. Safir. “ $B \rightarrow K^* \ell^+ \ell^- (\rho \ell \nu_\ell)$ Helicity Analysis in the LEET”. In: *European Physical Journal C* 25.4 (2002), pp. 583–601.
- [69] S. Rai Choudhury. “ $B \rightarrow K_1(1270) (\rho K) \ell^+ \ell^-$ in LEET”. In: *The European Physical Journal C* 58 (2008), pp. 251–259.
- [70] J. Charles. “Heavy to Light Form Factors in the Final Hadron Large Energy Limit of QCD”. In: *Physical Review D* 60 (1999).
- [71] Kenneth Wilson. “The Renormalization Group and the ϵ Expansion”. In: *Physics Reports* 12.2 (1974), pp. 75–199.
- [72] Stephen Olsen. “History of Belle and Some of its Lesser Known Highlights”. In: *International Workshop: High Energy Physics and Quantum Field Theory* 1 (2015).
- [73] The BaBar Collaboration. “The BaBar Detector”. In: *Nuclear Instruments and Methods in Physics Research Section A: Accelerators, Spectrometers, Detectors and Associated Equipment* 479.1 (2002), pp. 1–116.
- [74] Clara Moskowitz. “2 Accelerators Find Particles That May Break Known Laws of Physics”. In: *Scientific American* (2015).
- [75] R. Aaij. “Measurement of the Ratio of Branching Fractions $\mathcal{B}(\bar{B}^0 \rightarrow D^{*+} \tau^- \bar{\nu}_\tau) / \mathcal{B}(\bar{B}^0 \rightarrow D^{*+} \mu^- \bar{\nu}_\mu)$ ”. In: *Physical Review Letters* 115.11 (2015).
- [76] M. Huschle. “Measurement of the Branching Ratio $\bar{B} \rightarrow D^* \tau^- \bar{\nu}_\tau$ Relative to $\bar{B} \rightarrow D^* \ell^- \bar{\nu}_\ell$ Decays with Hadronic Tagging at Belle”. In: *Physical Review D* 92.7 (2015).
- [77] The ATLAS Collaboration. “The ATLAS Experiment at the CERN Large Hadron Collider”. In: *Journal of Instrumentation* 3 (2008).

- [78] N. V. Krasnikov. “The Search for New Physics at the LHC”. In: *Theoretical and Mathematical Physics* 132.3 (2002), pp. 1189–1200.
- [79] N. V. Krasnikov. “Physics at LHC”. In: *Physics of Particles and Nuclei Letters* 28 (1997), pp. 441–470.
- [80] Raymond Mountain. “Roadmap for Selected Key Measurements of LHCb”. In: *LHCb Public Notes* (2010).
- [81] The LHCb Collaboration. “Physics Case for an LHCb Upgrade II Opportunities in Flavour Physics, and beyond, in the HL-LHC Era”. In: *LHCb Public Notes* (2018).
- [82] R. Fulton. “Observation of B Meson Semileptonic Decays to Noncharmed Final States”. In: *Physical Review Letters* 64.1 (1990), pp. 16–20.
- [83] H. Albrecht. “Observation of B^0 - \bar{B}^0 Mixing”. In: *Physics Letters B* 192 (1987), pp. 369–376.